doi.org/10.36721/PJPS.2026.39.10.287.1

NOX4 promotes wear particle-stimulated inflammation and osteolysis by ROS-dependent NLRP3 inflammasome activation

Changming Xu, Lei Jiang and Hu Da*
Department of Orthopedics, Lianshui County People's Hospital, Huai'an, Jiangsu, China

Abstract: **Background**: Periprosthetic osteolysis (PIO) induced by wear particles is a major cause of implant failure, yet the underlying molecular mechanisms remain incompletely understood. Oxidative stress and inflammation are key pathological features, but the role of nicotinamide adenine dinucleotide phosphate oxidase 4 (NOX4) in this process is unclear. **Objectives**: This study aimed to investigate the role and mechanism of NOX4 in wear particle-stimulated inflammation and osteolysis, with a focus on the reactive oxygen species (ROS)/NLRP3 inflammasome signaling pathway. **Methods**: *In-vivo* and *in-vitro* PIO models were established using mice and Raw264.7 cells stimulated with cobalt-chromium-molybdenum alloy (Co-Cr-Mo) particles. NOX4 expression, inflammatory factor levels (TNF-α, IL-1β, IL-6), ROS production, and NLRP3 inflammasome activation (NLRP3, ASC, Caspase-1) were examined. The effects of NOX4 silencing, along with NLRP3 and ROS inhibition, were assessed. **Results**: Relative to normal mice and control group, the levels of inflammatory factors and NOX4 expression in PIO mice and cobalt-chromium-molybdenum alloy (Co-Cr-Mo)-stimulated Raw264.7 cells were higher. After NOX4 silencing, the levels of inflammatory factors in Raw264.7 cells were lower under situation of Co-Cr-Mo stimulation. The elevated NLRP3 inflammasome activation and ROS level caused by Co-Cr-Mo stimulation were reversed following NOX4 silencing. Co-Cr-Mo elevated the levels of NLRP3, apoptosis-associated speck-like protein containing a CARD (ASC) and Caspase-1 levels, but this effect was reversed after NOX4 silencing. NLRP3 inflammasome inhibitor or ROS inhibitor could reverse the elevated inflammation in Raw264.7 cells under Co-Cr-Mo stimulation. **Conclusion**: NOX4 promotes wear particle-induced inflammation and osteolysis by activating the ROS-dependent NLRP3 inflammasome, providing new targets for treating periprosthetic osteolysis.

Keywords: Inflammation; NOX4; NLRP3; Periprosthetic osteolysis; Particle; ROS

Submitted on 21-02-2025 – Revised on 01-07-2025 – Accepted on 07-07-2025

INTRODUCTION

Artificial joint replacement is an effective method for treating various end-stage joint diseases (Humphreys *et al.*, 2020), but peri-implant osteolysis (PIO) and aseptic loosening are the most common complications, which may lower patients' quality of life and increase the risk of instability (Chen *et al.*, 2023). Additionally, the underlying mechanism of PIO has not been completely clarified, elevating the difficulty of treating PIO (Qiu *et al.*, 2020).

Moreover, studies have manifested that the pathogenesis of aseptic loosening is strongly related to the inflammatory interface generated by macrophages and cytokines around the joint prosthesis and wear particles (Xu *et al.*, 2021). A growing body of literature has unveiled that the activation of the monocyte-macrophage system stimulated by wear particles promotes the release of proinflammatory chemokines, thus creating a favorable environment for osteoclast formation and original osteoclast activation, ultimately leading to osteolysis and aseptic loosening (Connors *et al.*, 2022).

As a member of the NOX family, nicotinamide adenine dinucleotide phosphate oxidase 4 (NOX4) can be stimulated during many cell differentiation processes (Liu *et al.*, 2023). Emerging evidence has indicated that NOX4 can produce reactive oxygen species (ROS) (Park *et al.*, 2021). More importantly, NOX4 exhibits persistent activity and can produce H_2O_2 even in the absence of cytosolic activator proteins (Pena *et al.*, 2022). This phenomenon has been proven to contribute to the formation of aseptic loosening (Xie *et al.*, 2023). In addition, it has been revealed that in mice with NOX4 knockout, the expression levels of markers for osteoclastogenesis and the bone resorption cycle were both reduced (Pan *et al.*, 2022). However, the relevant mechanism of NOX4 in particle-induced inflammatory osteolysis remains unclear.

The nucleotide-binding domain (NBD), leucine-rich repeat (LRR) and pyrin domain (PYD)-containing protein 3 (NLRP3) inflammasome is a critical part of the innate immune system. Relevant studies have shown that the NLRP3 inflammasome is associated with the formation of inflammatory osteolysis triggered by debris from wear and tear and is involved in the release process of inflammatory factors (Wu *et al.*, 2022). As reported previously, titanium particles can induce ROS production and cause structural changes in mitochondria. This indicates that drug therapies that inhibit the NLRP3 inflammasome represent a promising strategy for treating osteolysis caused by wear particle stimulation (Zheng *et al.*, 2021).

The aim of this research was to explore the potential role of NOX4 in wear particle-stimulated inflammation and osteolysis and to reveal its potential mechanism.

**Corresponding author:* e-mail: dahumd@sina.com

MATERIALS AND METHODS

Particle

DePuy (Raynham, MA, USA) provided cobalt-chromium-molybdenum alloy (Co-Cr-Mo) particles. Particles were treated in 70% ethanol solution with shaking for one night, followed by washing and suspending in sterile PBS to a final concentration of 3×10^9 particles/ ml.

Establishment of PIO mice model

Suzhou Healthytech Bio-pharmaceutical Co., Ltd. (Suzhou, China) provided 12 female C57BL/J6 mice (8-week-old), followed by randomly dividing them into a normal group and a PIO group and each group had 6 mice. For PIO mice, an ophthalmological scalpel was adopted to create a sagittal incision above the calvarium (Huang *et al.*, 2025). Meanwhile, 30 μl of particle suspensions were implanted into the surface of bilateral parietal bones and the periosteum was removed. The normal mice also underwent the same surgery, in which 30 microliters of sterile normal saline without any particles was implanted. After 14 days, all mice were sacrificed by carbon dioxide (CO_2) inhalation using a custom-designed 5 L CO_2 inhalation chamber (controlled gas flow at 20% chamber volume per minute) for harvesting the cranium for isolation. All animal procedures were performed in accordance with institutional guidelines for the care and use of laboratory animals, and every effort was made to minimize suffering.

Sample size calculation

Power analysis was carried out in this study using G*Power 3.1.9.7 software (Heinrich Heine University Düsseldorf, Germany) to determine the sample size required to detect statistical differences (Kang, 2021). With an alpha level of 0.05 and 90% power analysis, the research revealed that a sample size of 6 mice per group was required. Therefore, to draw reliable conclusions, the study sample sizes were 6 mice per group.

Cell culture, transfection and treatment

American Type Culture Collection (ATCC, Manassas, VA, USA) provided the Raw264.7 mouse macrophage cell line, which was maintained in RPMI 1640 medium containing 10% fetal bovine serum (FBS, Thermo Fisher Scientific, Waltham, MA, USA) in 5% CO_2 incubator at 37°C. Transfection of 2 shRNAs targeting NOX4 and negative controls (Invitrogen, Carlsbad, CA, USA) in cells was implemented by means of Lipofectamine 2000 reagent (Invitrogen, Carlsbad, CA, USA). In addition, cells were exposed to Co-Cr-Mo alloy particles (2 mg/ml) for 48 h (Zheng *et al.*, 2018). Besides, an NLRP3 inflammasome inhibitor (BAY11-7082, Selleck Chemicals, Houston, TX, USA) was utilized at a concentration of 5 μM. The ROS inhibitor N-acetylcysteine (NAC, Sigma-Aldrich, St. Louis, MO, USA) was utilized at a concentration of 10 mM.

RT-qPCR

Total RNA was extracted from tissues or cells with the help of Trizol Kit (Invitrogen, Carlsbad, CA, USA). The synthesis of complementary DNA (cDNA) was implemented by RevertAid First Strand cDNA Synthesis Kit (Invitrogen, Carlsbad, CA, USA) from total RNA. Then, quantitative PCR was implemented using the iTaq™ Universal SYBR® Green Supermix kit (Bio-Rad Laboratories, Hercules, CA, USA) on a Bio-Rad CFX96 Touch Real-Time PCR Detection System (Bio-Rad Laboratories, USA). The gene expression was measured by $2^{-\Delta\Delta Ct}$ method. GAPDH was adopted as an internal control (Pan *et al.*, 2023).

Enzyme-linked immunosorbent assay (ELISA)

The concentrations of TNF-α, IL-1β, and IL-6 in tissues and cells were tested by the corresponding ELISA kits (R&D Systems, Minneapolis, MN, USA). The absorbance at 450 nm was measured using a BioTek Synergy H1 microplate reader (Agilent Technologies, Santa Clara, CA, USA) as described previously (Liu *et al.*, 2020).

Immunofluorescence (IF)

Cells growing on glass coverslips were planted into the 6-well plates for one night. Followed by washing, cells were fixed with 4% formaldehyde as well as permeabilized with 0.2% Triton X-100. Next, cells were cultivated with NLRP3 primary antibody and ASC primary antibody (both from Cell Signaling Technology, Danvers, MA, USA) at 4ºC for one night. Followed by washing, cells were cultivated with fluorescence secondary antibody (Alexa Fluor 488, Invitrogen, USA), mounted with 95% glycerin and imaged using an Olympus IX83 fluorescence microscope (Olympus Corporation, Tokyo, Japan) equipped with a DP80 digital camera (Olympus, Japan) (Huang *et al.*, 2023).

DCFH-DA

ROS were tested by means of the DCFH-DA probe (Beyotime Biotechnology, Shanghai, China) (Yang *et al.*, 2024). Briefly, cells were planted into the 12-well plates for one night of culture. Then, cells were cultivated with the DCFH-DA probe for 30 min. After washing, the ROS staining was observed under the Olympus IX83 fluorescence microscope (Olympus Corporation, Japan).

Western-blot

First, the cells and tissues were lysed using the RIPA lysis buffer (Bio-Techne, Minneapolis, MN, USA) and the total protein concentration was determined using the BCA protein assay kit (Bio-Techne, USA). Then, the proteins were separated by SDS-PAGE using a Bio-Rad Mini-PROTEAN Tetra electrophoresis system (Bio-Rad Laboratories, USA) and transferred onto PVDF membranes using a Bio-Rad Trans-Blot Turbo transfer system (Bio-Rad Laboratories, USA). The membrane was sealed with 5% skimmed milk for two hours and then an overnight incubation with the primary antibody (all from Abcam, Cambridge, MA, USA) was performed at 4°C. Subsequently, the membrane was washed with HRP-conjugated secondary antibodies (Abcam, USA). Protein

bands were visualized using the enhanced chemiluminescence (ECL) method (Bio-Rad Clarity Western ECL Substrate, Bio-Rad Laboratories, USA) and imaged using a Tanon 5200 Multi chemiluminescence imaging system (Tanon Science & Technology, Shanghai, China) (Yu *et al.*, 2024).

Statistical analysis

SPSS 22.0 software (IBM Corporation, Armonk, NY, USA) was used for data analysis. Data were presented as the mean ± standard deviation (SD) and analyzed using Student's t-test (for two-group comparisons) or one-way analysis of variance (ANOVA) followed by Tukey's post-hoc test (for multiple-group comparisons). All experiments were performed in triplicate, and each independent experiment was repeated at least three times. A p-value < 0.05 was considered statistically significant.

RESULTS

Inflammation and NOX4 expression in PIO mice

To determine inflammation as well as NOX4 expression in PIO mice, wear particles were implanted on the exposed periosteum of mouse calvaria to induce osteolysis. Relative to normal mice, TNF-a, IL-1β, as well as IL-6 levels in PIO mice presented elevation (Fig. 1A-1C). Besides, NOX4 was up-regulated in PIO mice compared to normal mice (Figs. 1D-1F).

Inflammation and NOX4 expression in Raw264.7 cells under situation of Co-Cr-Mo stimulation

Raw264.7 cells were stimulated with Co-Cr-Mo to imitate PIO *in-vitro*. In contrast to the control group, TNF-α, IL-1β, as well as IL-6 levels were elevated in Raw264.7 cells under the situation of Co-Cr-Mo stimulation (Fig. 2A-2C). Meanwhile, NOX4 expression was up-regulated in Raw264.7 cells under the situation of Co-Cr-Mo stimulation (Fig. 2D-2F).

NOX4 promotes inflammation in Raw264.7 cells under Co-Cr-Mo stimulation

To investigate whether NOX4 participated in inflammation, RAW264.7 cells were transfected with shRNAs targeting NOX4. RT-qPCR and Western blot verified the successful transfection of sh-NOX4#1/#2 (fig. 3A-3C). According to Fig. 3D-3F, TNF-a, IL-1β and IL-6 levels in Raw264.7 cells were up-regulated after Co-Cr-Mo treatment and after transfection with sh-NOX4#1/#2, their levels were significantly declined.

NOX4 promotes NLRP3 inflammasome activation and ROS level in Raw264.7 cells under situation of Co-Cr-Mo stimulation

Through IF staining, Co-Cr-Mo facilitated the fluorescence intensity of NLRP3 and ASC, but NOX4 silencing reduced the fluorescence intensity of NLRP3 and ASC under situation of Co-Cr-Mo (Fig. 4A). In ROS detection, ROS level was enhanced in Raw264.7 cells followed by Co-Cr-Mo treatment, but further lessened after NOX4 silencing (Fig. 4B). Western blot also suggested that Co-Cr-Mo elevated NLRP3, ASC and Caspase-1 levels, but this effect was reversed upon NOX4 silencing (Fig. 4C-4F).

Repression of NLRP3 inflammasome and ROS production inhibits inflammation in Raw264.7 cells under Co-Cr-Mo stimulation

In the next experiments, NLRP3 inflammasome inhibitor (BAY11-7082) and ROS inhibitor (NAC) were used to assess the impacts of ROS and NLRP3 inflammasome on the inflammation in Co-Cr-Mo-stimulated Raw264.7 cells. It was revealed that BAY11-7082 or NAC could reverse the elevated levels of inflammatory factors in Raw264.7 cells under Co-Cr-Mo stimulation (Figs. 5A-5C). Meanwhile, the enhanced NLRP3 and ASC levels in Raw264.7 cells could be offset after BAY11-7082 or NAC treatment under Co-Cr-Mo stimulation (Fig. 5D). Besides, the elevated ROS level in Raw264.7 cells was rescued after BAY11-7082 or NAC treatment under Co-Cr-Mo stimulation (Fig. 5E). Moreover, the elevated NLRP3, ASC and Caspase-1 levels in Raw264.7 cells could be counteracted after BAY11-7082 or NAC treatment under Co-Cr-Mo stimulation (Fig. 5F-5I).

DISCUSSION

As one of the common complications of total joint replacement, aseptic loosening may lead to the need for another surgery, increase medical costs, prolong hospital stay and also aggravate the economic burden of the patients (Sun *et al.*, 2023). Previous studies have confirmed that inflammation caused by wear particles plays a crucial role in the pathogenesis of osteolysis and aseptic loosening (Hodges *et al.*, 2021). Furthermore, the presence of wear particles can lead to the phagocytic action of macrophages, which prompts mononuclear macrophages to differentiate into functional osteoclasts and produce inflammatory mediators (Cong *et al.*, 2023). In this research, the levels of inflammatory factors were also assessed to verify the presence of inflammation both *in-vivo* and *in-vitro*, which was consistent with previous reports (Hodges *et al.*, 2021, Sun *et al.*, 2023).

The NOX gene family consists of seven members, containing NOX1-NOX5, DUOX1, as well as DUOX2 (Vermot *et al.*, 2021). NOX4 is involved in the pathological processes of many diseases, such as atherosclerosis, diabetic nephropathy, pulmonary fibrosis, cancer and neurodegenerative diseases (Blaskovic *et al.*, 2021, Szczepaniak *et al.*, 2022, Boonpraman *et al.*, 2023, Wang *et al.*, 2023). It is worth noting that NOX4 is particularly associated with osteoporosis, inflammatory arthritis and osteoarthritis (Cao *et al.*, 2022, Zhou *et al.*, 2022, Huang *et al.*, 2023). Intriguingly, the research shows that the expression level of NOX4 is elevated in the clinical tissues of patients who have undergone artificial joint replacement surgery.

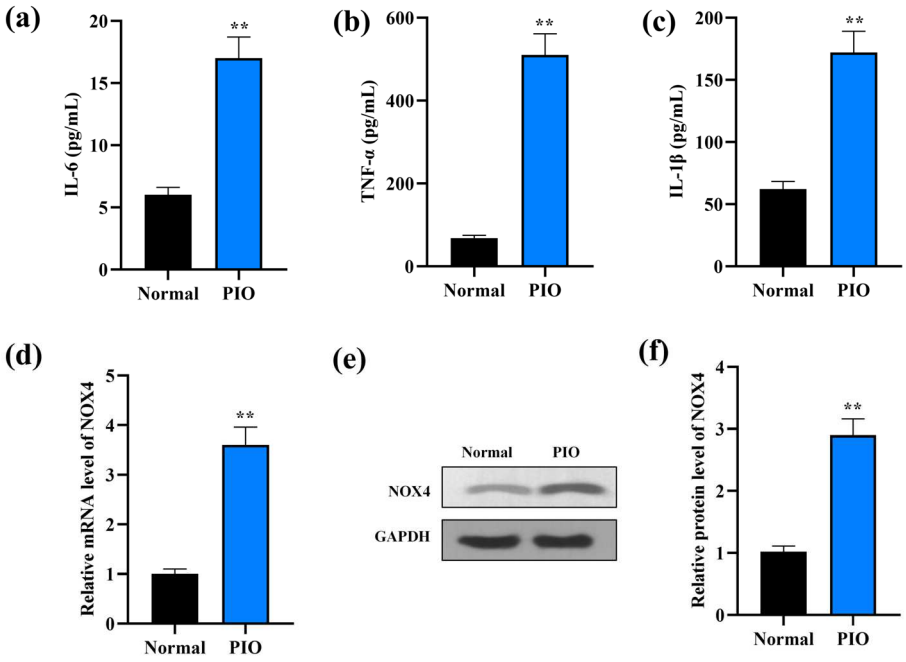

Fig. 1: Inflammation and NOX4 expression in PIO mice.
(a) IL-6 levels in normal mice and PIO mice were examined by ELISA. (b) TNF-α levels in normal mice and PIO mice were examined by ELISA. (c) IL-1β levels in normal mice and PIO mice were examined by ELISA. (d) Relative mRNA levels of NOX4 in normal mice and PIO mice were detected by RT-qPCR. (e) Western blot analysis of protein levels of NOX4 in normal mice and PIO mice. (f) Protein quantification level of NOX4 in normal mice and PIO mice. $^{**}P<0.01$. IL-6: Interleukin-6; TNF-α: Tumor necrosis factor-α; IL-1β: Interleukin-1β; PIO: Periprosthetic osteolysis; NOX4: Nicotinamide adenine dinucleotide phosphate oxidase 4; GAPDH: Glyceraldehyde 3-phosphate dehydrogenase.

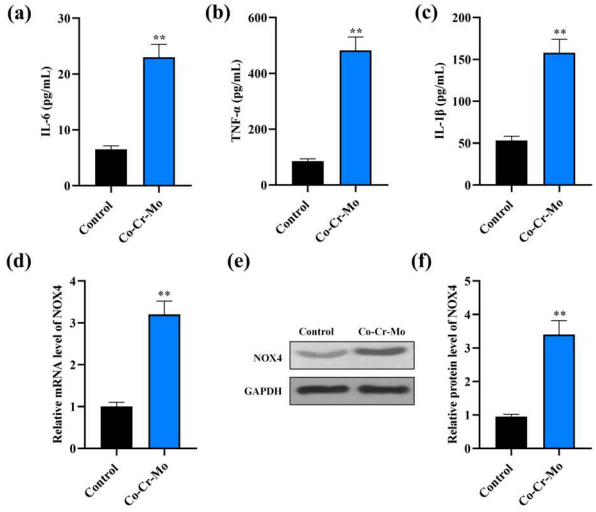

Fig. 2: Inflammation and NOX4 expression in Co-Cr-Mo treated Raw264.7 cells.
(a) IL-6 levels in Co-Cr-Mo treated Raw264.7 cells were examined by ELISA. (b) TNF-α levels in Co-Cr-Mo treated Raw264.7 cells were examined by ELISA. (c) IL-1β levels in Co-Cr-Mo treated Raw264.7 cells were examined by ELISA. (d) Relative mRNA levels of NOX4 in Co-Cr-Mo treated Raw264.7 cells were tested by RT-qPCR. (e) Western blot analysis of protein levels of NOX4 in Co-Cr-Mo treated Raw264.7 cells. (f) Protein quantification level of NOX4 in Co-Cr-Mo treated Raw264.7 cells. $^{**}P<0.01$. IL-6: Interleukin-6; TNF-α: Tumor necrosis factor-α; IL-1β: Interleukin-1β; Co-Cr-Mo: Cobalt-chromium-molybdenum alloy; NOX4: Nicotinamide adenine dinucleotide phosphate oxidase 4; GAPDH: Glyceraldehyde 3-phosphate dehydrogenase.

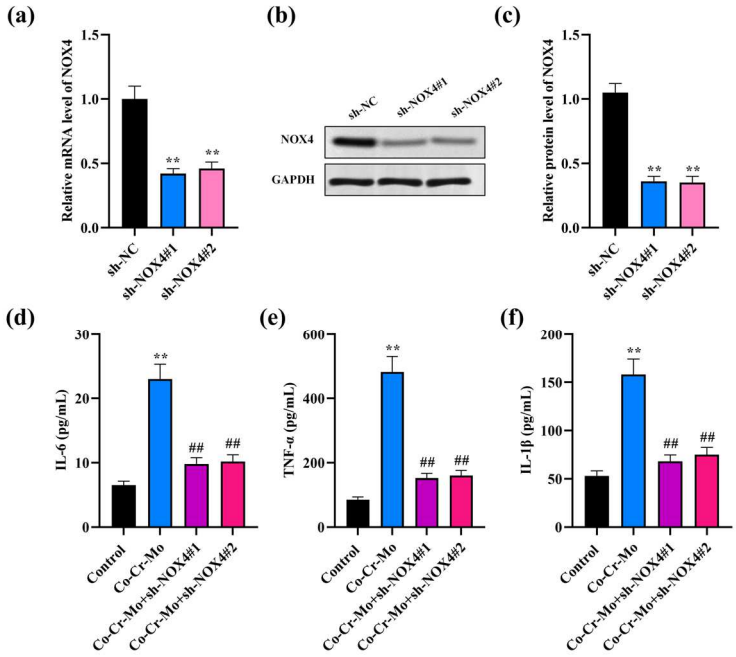

Fig. 3: NOX4 promotes inflammation in Co-Cr-Mo treated Raw264.7 cells.
(a) RT-qPCR verified the transfection efficiency of sh-NOX4#1 and sh-NOX4#2. (b) Western blot verified the transfection efficiency of sh-NOX4#1 and sh-NOX4#2. (c) Protein quantification level of NOX4. (d) IL-6 levels in Co-Cr-Mo treated Raw264.7 cells were examined by ELISA after transfection of sh-NOX4#1 and sh-NOX4#2. (e) TNF-α levels in Co-Cr-Mo treated Raw264.7 cells were examined by ELISA after transfection of sh-NOX4#1 and sh-NOX4#2. (f) IL-1β levels in Co-Cr-Mo treated Raw264.7 cells were examined by ELISA after transfection of sh-NOX4#1 and sh-NOX4#2. $^{**}P<0.01$. IL-6: Interleukin-6; TNF-α: Tumor necrosis factor-α; IL-1β: Interleukin-1β; Co-Cr-Mo: Cobalt-chromium-molybdenum alloy; NOX4: Nicotinamide adenine dinucleotide phosphate oxidase 4; GAPDH: Glyceraldehyde 3-phosphate dehydrogenase.

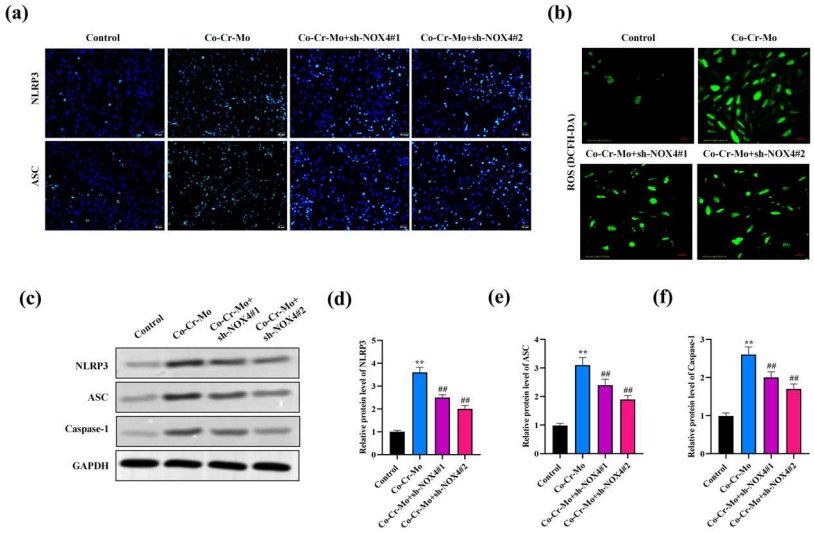

Fig. 4: NOX4 promotes NLRP3 inflammasome activation and ROS level in Co-Cr-Mo treated Raw264.7 cells.
(a) IF staining examined the levels of NLRP3 and ASC in Co-Cr-Mo treated Raw264.7 cells in the presence of NOX4 silence. (b) ROS level in Co-Cr-Mo treated Raw264.7 cells in the presence of NOX4 silence. (c) Western blot measured the levels of NLRP3, ASC and Caspase-1 in Co-Cr-Mo treated Raw264.7 cells in the presence of NOX4 silence. (d) Protein quantification level of NLRP3. (e) Protein quantification level of ASC. (f) Protein quantification level of Caspase-1. $^{**}P<0.01$. Co-Cr-Mo: Cobalt-chromium-molybdenum alloy; NOX4: Nicotinamide adenine dinucleotide phosphate oxidase 4; GAPDH: Glyceraldehyde 3-phosphate dehydrogenase; ASC: Apoptosis-associated speck-like protein containing a CARD; NLRP3: NOD-like receptor family, pyrin domain containing protein 3; ROS: Reactive oxygen species; DCFH-DA: 2',7'-Dichlorodihydrofluorescein diacetate; Caspase-1: Cysteine-requiring aspartate protease-1.

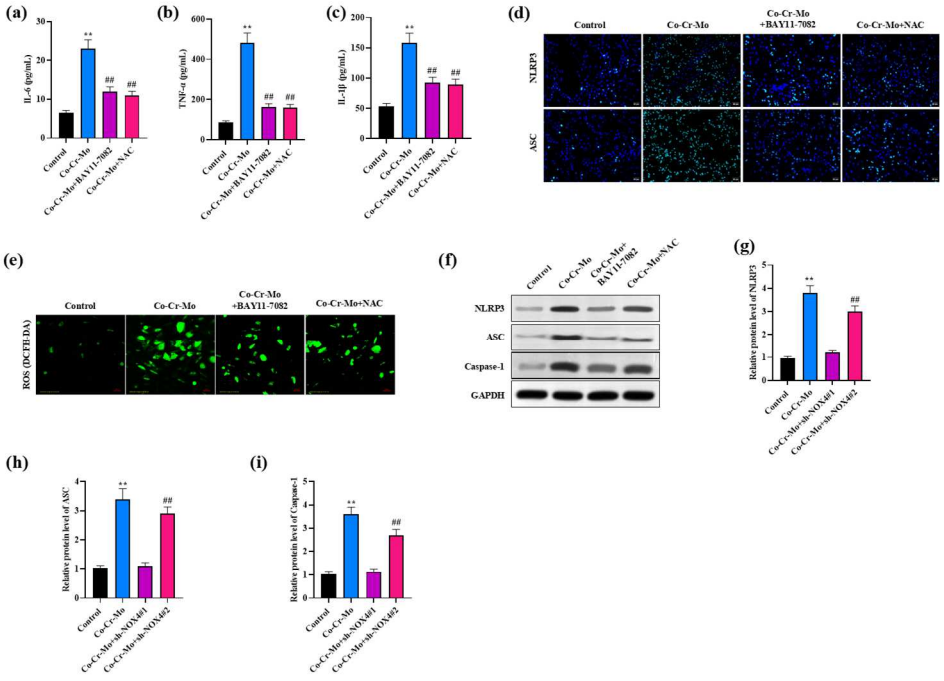

Fig. 5: Inhibition of NLRP3 inflammasome and ROS production inhibits the release of inflammatory factors in Co-Cr-Mo treated Raw264.7 cells.

(a) IL-6 levels in different groups (Control, Co-Cr-Mo, Co-Cr-Mo+BAY11-7082, and Co-Cr-Mo+NAC) were examined by ELISA. (b) TNF-a levels in different groups (Control, Co-Cr-Mo, Co-Cr-Mo+BAY11-7082, and Co-Cr-Mo+NAC) were examined by ELISA. (c) IL-1β levels in different groups (Control, Co-Cr-Mo, Co-Cr-Mo+BAY11-7082, and Co-Cr-Mo+NAC) were examined by ELISA. (d) IF staining examined the levels of NLRP3 and ASC in different groups (Control, Co-Cr-Mo, Co-Cr-Mo+BAY11-7082, and Co-Cr-Mo+NAC). (e) ROS level in different groups (Control, Co-Cr-Mo, Co-Cr-Mo+BAY11-7082, and Co-Cr-Mo+NAC). (f) Western blot measured the levels of NLRP3, ASC and Caspase-1 in different groups (Control, Co-Cr-Mo, Co-Cr-Mo+BAY11-7082, and Co-Cr-Mo+NAC). (g) Protein quantification level of NLRP3. (h) Protein quantification level of ASC. (i) Protein quantification level of Caspase-1. $^{**}P<0.01$, compared with control group. $^{\#\#}P<0.01$, compared with Co-Cr-Mo group. IL-6: Interleukin-6; TNF-α: Tumor necrosis factor-α; IL-1β: Interleukin-1β; Co-Cr-Mo: Cobalt-chromium-molybdenum alloy; GAPDH: Glyceraldehyde 3-phosphate dehydrogenase; ASC: Apoptosis-associated speck-like protein containing a CARD; NLRP3: NOD-like receptor family, pyrin domain containing protein 3; ROS: Reactive oxygen species; DCFH-DA: 2',7'-Dichlorodihydrofluorescein diacetate; Caspase-1: Cysteine-requiring aspartate protease-1.

This indicates that NOX4 plays a crucial role in PIO (Wang *et al.*, 2022). Consistently, NOX4 was observed to be up-regulated in PIO mice and Co-Cr-Mo-stimulated Raw264.7 cells. More importantly, NOX4 silencing could repress wear particle-stimulated inflammation and osteolysis. Similarly, Wang *et al.* proved that NOX4 reduction suppressed titanium nanoparticle-stimulated bone destruction, implying that NOX4 repression may be a promising therapeutic method for restraining periprosthetic osteolysis (Wang *et al.*, 2022).

NOX4 is also regarded as a regulatory enzyme of ROS and it plays a crucial role in various oxidative stress responses (Huang *et al.*, 2023). NOX4 can catalyze the oxidation process to produce a large amount of ROS. These ROS can enhance the activation of the NLRP3 inflammasome, thereby promoting the inflammatory response (Li *et al.*, 2022). ROS is usually composed of superoxide anions, hydrogen peroxide, as well as hydroxyl radicals, which are involved in regulating cell survival, proliferation, metabolism, as well as differentiation (Cheung *et al.*, 2022). It is worth noting that under the stimulation of nanoparticles, the generation of ROS in the microenvironment around the implant will significantly increase. This will accelerate the maturation of osteoclasts in the surrounding bone tissue and the process of surface bone destruction, ultimately leading to the occurrence of bone resorption (Wei *et al.*, 2022). Therefore, modulating the excessive ROS production may be an effective strategy for treating PIO (Zhang *et al.*, 2022).

The NLRP3 inflammasome plays a negative role in the inflammatory response of osteoblasts and studies have confirmed its association with osteolysis triggered by debris from wear (Wang *et al.*, 2023). NOX4 was confirmed to promote NLRP3 inflammasome activation and ROS level in Raw264.7 cells under situation of Co-Cr-Mo stimulation. Besides, inhibition of NLRP3

inflammasome or ROS level inhibited the levels of inflammatory factors in Co-Cr-Mo-stimulated Raw264.7 cells, which proved ROS-dependent NLRP3 inflammasome activation was a downstream signaling of NOX4. Thus, NOX4 may be a crucial factor implicated in wear particle-stimulated inflammation along with osteolysis.

This study has some limitations. Firstly, this study relies on the RAW264.7 macrophage (*in-vitro* experiment) as the prerequisite condition. Secondly, this research lacks clinical validation. Additionally, the discussion section did not conduct a long-term result analysis. Therefore, in the future, clinical experiments will be conducted to analyze the long-term role of NOX4 in periprosthetic osteolysis.

CONCLUSION

In conclusion, this study demonstrates that NOX4 facilitates wear particle-stimulated inflammation along with osteolysis by ROS-dependent NLRP3 inflammasome activation, providing novel targets for treating periprosthetic osteolysis.

Acknowledgements
None.

Authors' contributions
Changming Xu and Lei Jiang: Designed the study and wrote the main manuscript text; Changming Xu and Hu Da: Performed the *in-vivo* experiments and analyzed the data; Lei Jiang and Hu Da: Conducted the *in-vitro* cell studies and prepared figures; Changming Xu and Hu Da: Supervised the project and revised the manuscript. All authors reviewed and approved the final version of the manuscript.

Funding
There was no funding.

Data availability statement
The datasets generated and/or analyzed during the current study are available from the corresponding author upon reasonable request.

Ethical approval
This study was approved by the Ethics Committee of Lianshui County People's Hospital (Approval number: 2021-014). All animal procedures were performed in accordance with the approved guidelines and regulations, and every effort was made to minimize animal suffering. This study was performed in adherence with the ARRIVE guidelines. See supplementary file for the ARRIVE checklist.

Conflict of interest
The authors declare no conflict of interest.

Supplementary data
https://www.pjps.pk/uploads/2026/07/SUP1783418516.pdf

REFERENCES

Blaskovic S, Donati Y, Ruchonnet-Metrailler I, Seredenina T, Krause KH, Pache JC, Adler D, Barazzone-Argiroffo C and Jaquet V (2021). Di-tyrosine crosslinking and nox4 expression as oxidative pathological markers in the lungs of patients with idiopathic pulmonary fibrosis. *Antioxidants (Basel).* **10**(11):1833.

Boonpraman N, Yoon S, Kim CY, Moon JS and Yi SS (2023). NOX4 as a critical effector mediating neuroinflammatory cytokines, myeloperoxidase and osteopontin, specifically in astrocytes in the hippocampus in Parkinson's disease. *Redox Biol.* **62**: 102698.

Cao Z, Liu G, Zhang H, Wang M and Xu Y (2022). Nox4 promotes osteoblast differentiation through TGF-beta signal pathway. *Free Radic Biol Med.* **193**(Pt 2): 595-609.

Chen L, Tong Z, Luo H, Qu Y, Gu X and Si M (2023). Titanium particles in peri-implantitis: distribution, pathogenesis and prospects. *Int J Oral Sci.* **15**(1): 49.

Cheung EC and Vousden KH (2022). The role of ROS in tumour development and progression. *Nat Rev Cancer.* **22**(5): 280-297.

Cong Y, Wang Y, Yuan T, Zhang Z, Ge J, Meng Q, Li Z and Sun S (2023). Macrophages in aseptic loosening: Characteristics, functions, and mechanisms. *Front Immunol.* **14**: 1122057.

Connors JP, Stelzer JW, Garvin PM, Wellington IJ and Solovyova O (2022). The role of the innate immune system in wear debris-induced inflammatory Peri-implant osteolysis in total joint arthroplasty. *Bioengineering (Basel).* **9**(12).

Hodges NA, Sussman EM and Stegemann JP (2021). Aseptic and septic prosthetic joint loosening: Impact of biomaterial wear on immune cell function, inflammation, and infection. *Biomaterials.* **278**: 121127.

Huang C, Zhang C, Luo Y, Guo L, Wu Y, Shi Q, Zhang Y, Yang C, Wang B, Niu J and Lin J (2025). The flavonoid kaempferol mitigates periprosthetic osteolysis by regulating the NLRP3 Inflammasome and balancing Bone Metabolism. *J Cell Mol Med.* **29**(19): e70878.

Huang X, Ye C, Zhao X, Tong Y, Lin W, Huang Q, Zheng Y, Wang J, Zhang A and Mo Y (2023). TRIM45 aggravates microglia pyroptosis via Atg5/NLRP3 axis in septic encephalopathy. *J Neuroinflammation.* **20**(1): 284.

Huang YF, Wang G, Ding L, Bai ZR, Leng Y, Tian JW, Zhang JZ, Li YQ, Ahmad, Qin YH, Li X and Qi X (2023). Lactate-upregulated NADPH-dependent NOX4 expression via HCAR1/PI3K pathway contributes to ROS-induced osteoarthritis chondrocyte damage. *Redox Biol.* **67**: 102867.

Humphreys H and Hoffman P (2020). The conundrum of ultraclean air, deep infections, and artificial joint replacement. *J Hosp Infect.* **104**(1): 123-124.

Kang H (2021). Sample size determination and power analysis using the G*Power software. *J Educ Eval Health Prof.* **18**: 17.

Li Q, Hua X, Li L, Zhou X, Tian Y, Deng Y, Zhang M, Yuan X and Chi W (2022). AIP1 suppresses neovascularization by inhibiting the NOX4-induced NLRP3/NLRP6 imbalance in a murine corneal alkali burn model. *Cell Commun Signal.* **20**(1): 59.

Liu L, Zhou M, Zhu R, Zhou J, Ni L, Wang Z, Liu N, Zhu F, Shi T, Deng Z, Wang Y, Tian Y, Li R, Yang H, Wang Z, Jiang J and Xu Y (2020). Hydrogen sulfide protects against particle-induced inflammatory response and osteolysis via SIRT1 pathway in prosthesis loosening. *Faseb j.* **34**(3): 3743-3754.

Liu WJ, Wang L, Zhou FM, Liu SW, Wang W, Zhao EJ, Yao QJ, Li W, Zhao YQ, Shi Z, Qiu JG and Jiang BH (2023). Elevated NOX4 promotes tumorigenesis and acquired EGFR-TKIs resistance via enhancing IL-8/PD-L1 signaling in NSCLC. *Drug Resist Updat.* **70**: 100987.

Pan B, Zhang Z, Wu X, Xian G, Hu X, Gu M, Zheng L, Li X, Long L, Chen W and Sheng P (2023). Macrophage-derived exosomes modulate wear particle-induced osteolysis via miR-3470b targeting TAB3/NF-κB signaling. *Bioact Mater.* **26**: 181-193.

Pan W, Zheng L, Gao J, Ye L, Chen Z, Liu S, Pan B, Fang J, Lai H, Zhang Y, Ni K, Lou C and He D (2022). SIS3 suppresses osteoclastogenesis and ameliorates bone loss in ovariectomized mice by modulating Nox4-dependent reactive oxygen species. *Biochem Pharmacol.* **195**: 114846.

Park MW, Cha HW, Kim J, Kim JH, Yang H, Yoon S, Boonpraman N, Yi SS, Yoo ID and Moon JS (2021). NOX4 promotes ferroptosis of astrocytes by oxidative stress-induced lipid peroxidation via the impairment of mitochondrial metabolism in Alzheimer's diseases. *Redox Biol.* **41**: 101947.

Pena E, El Alam S, Siques P and Brito J (2022). Oxidative stress and diseases associated with high-altitude exposure. *Antioxidants (Basel).* **11**(2): 267.

Qiu J, Peng P, Xin M, Wen Z, Chen Z, Lin S, Kuang M, Fu Y, Fang G, Li S, Li C, Mao J, Qin L and Ding Y (2020). ZBTB20-mediated titanium particle-induced peri-implant osteolysis by promoting macrophage inflammatory responses. *Biomater Sci.* **8**(11): 3147-3163.

Sun Z, Kang J, Yang S, Zhang Y, Huang N, Zhang X, Du G, Jiang J and Ning B (2023). CD73 inhibits titanium particle-associated aseptic loosening by alternating activation of macrophages. *Int Immunopharmacol.* **122**: 110561.

Szczepaniak P, Siedlinski M, Hodorowicz-Zaniewska D, Nosalski R, Mikolajczyk TP, Dobosz AM, Dikalova A, Dikalov S, Streb J, Gara K, Basta P, Krolczyk J, Sulicka-Grodzicka J, Jozefczuk E, Dziewulska A, Saju B, Laksa I, Chen W, Dormer J, Tomaszewski M, Maffia P, Czesnikiewicz-Guzik M, Crea F, Dobrzyn A, Moslehi J, Grodzicki T, Harrison DG and Guzik TJ (2022). Breast cancer chemotherapy induces vascular dysfunction and hypertension through a NOX4-dependent mechanism. *J Clin Invest.* **132**(13):e149117.

Vermot A, Petit-Härtlein I, Smith SME and Fieschi F (2021). NADPH Oxidases (NOX): An Overview from Discovery, Molecular Mechanisms to Physiology and Pathology. *Antioxidants (Basel).* **10**(6):890.

Wang D, Li J, Luo G, Zhou J, Wang N, Wang S, Zhao R, Cao X, Ma Y, Liu G and Hao L (2023). Nox4 as a novel therapeutic target for diabetic vascular complications. *Redox Biol.* **64**: 102781.

Wang W, Liang X, Liu X, Bai J, Zhang W, Li W, Wang T, Li M, Wu Z, Chen L, Yang H, Gu Y, Tao Y, Zhou J, Wang H and Geng D (2022). NOX4 blockade suppresses titanium nanoparticle-induced bone destruction via activation of the Nrf2 signaling pathway. *J Nanobiotechnology.* **20**(1): 241.

Wang Z, Zhou F, Feng X, Li H, Duan C, Wu Y and Xiong Y (2023). FoxO1/NLRP3 inflammasome promotes age-related alveolar bone resorption. *J Dent Res.* **102**(8): 919-928.

Wei L, Chen W, Huang L, Wang H, Su Y, Liang J, Lian H, Xu J, Zhao J and Liu Q (2022). Alpinetin ameliorates bone loss in LPS-induced inflammation osteolysis via ROS mediated P38/PI3K signaling pathway. *Pharmacol Res.* **184**: 106400.

Wu Y, Teng Y, Zhang C, Pan Y, Zhang Q, Zhu X, Liu N, Su X and Lin J (2022). The ketone body β-hydroxybutyrate alleviates CoCrMo alloy particles induced osteolysis by regulating NLRP3 inflammasome and osteoclast differentiation. *J Nanobiotechnology.* **20**(1): 120.

Xie J, Hu Y, Su W, Chen S, Wang J, Liang S, Chen M, Wang H and Ma T (2023). PLGA nanoparticles engineering extracellular vesicles from human umbilical cord mesenchymal stem cells ameliorates polyethylene particles induced periprosthetic osteolysis. *J Nanobiotechnology.* **21**(1): 398.

Xu Y, Sang W, Zhong Y, Xue S, Yang M, Wang C, Lu H, Huan R, Mao X, Zhu L, He C and Ma J (2021). CoCrMo-nanoparticles induced peri-implant osteolysis by promoting osteoblast ferroptosis via regulating Nrf2-ARE signalling pathway. *Cell Prolif.* **54**(12): e13142.

Yang R, Gao W, Wang Z, Jian H, Peng L, Yu X, Xue P, Peng W, Li K and Zeng P (2024). Polyphyllin I induced ferroptosis to suppress the progression of hepatocellular carcinoma through activation of the mitochondrial dysfunction via Nrf2/HO-1/GPX4 axis. *Phytomedicine.* **122**: 155135.

Yu X, Jiang J, Li C, Wang Y, Ren Z, Hu J, Yuan T, Wu Y, Wang D, Sun Z, Wu Q, Chen B, Fang P, Ding H, Meng J, Jiang H, Zhao J and Bao N (2024). Osthole ameliorates wear particle-induced osteogenic impairment by mitigating endoplasmic reticulum stress

via PERK signaling cascade. *Mol Med.* **30**(1): 266.

Zhang Y, Yan M, Niu W, Mao H, Yang P, Xu B and Sun Y (2022). Tricalcium phosphate particles promote pyroptotic death of calvaria osteocytes through the ROS/NLRP3/Caspase-1 signaling axis in amouse osteolysis model. *Int Immunopharmacol.* **107**: 108699.

Zheng DZ, Bu YM and Wang L (2018). miR-130b participates in wear particle-induced inflammation and osteolysis via FOXF2/NF-κB pathway. *Immunopharmacol Immunotoxicol.* **40**(5): 408-414.

Zheng K, Bai J, Li N, Li M, Sun H, Zhang W, Ge G, Liang X, Tao H, Xue Y, Hao Y, Zhu C, Xu Y and Geng D (2021). Protective effects of sirtuin 3 on titanium particle-induced osteogenic inhibition by regulating the NLRP3 inflammasome via the GSK-3β/β-catenin signalling pathway. *Bioact Mater.* **6**(10): 3343-3357.

Zhou R, Chen Y, Li S, Wei X, Hu W, Tang S, Ding J, Fu W, Zhang H, Chen F, Hao W, Lin Y, Zhu R, Wang K, Dong L, Zhao Y, Feng X, Chen F, Ding C and Hu W (2022). TRPM7 channel inhibition attenuates rheumatoid arthritis articular chondrocyte ferroptosis by suppression of the PKCα-NOX4 axis. *Redox Biol.* **55**: 102411.